Long, Needle-like Carbon Nanotubes and Asbestos Activate the NLRP3 Inflammasome through a Similar Mechanism

Jaana Palomäki,* Elina Välimäki, Jukka Sund, Minnamari Vippola, Per Axel Clausen, Keld Alstrup Jensen, Kai Savolainen, Sampsa Matikainen, and Harri Alenius

Unit of Immunotoxicology, Finnish Institute of Occupational Health, 00250, Helsinki, Finland

Carbon nanomaterials (CNM) have unique technical characteristics which have attracted the interest of manufacturers but have also raised concerns about their possible harmful health effects, especially through occupational exposures. In an ideal carbon nanotube, the sp^2-hybridized carbon atoms are arranged in a rolled-up-like graphene sheet that is welded into a seamless tube. CNT may be either single (single-walled carbon nanotubes; SCNT) or multiple layers thick (multiwalled carbon nanotubes, MCNT). The aspect ratio of CNT is high due to their nanoscale width compared to the fiber length which can be as long as several micrometers.[1] The needle-like shape of CNT resembles asbestos fibers, and this raises a spectre of possible adverse health effects such as chronic pulmonary inflammation, fibrosis, and mesothelioma, the cancer of the mesothelial lining.[2−4] These disease stages have previously been shown to be associated with exposure to asbestos. Poland and colleagues[2] reported that especially long (>5 μm), needle-like carbon nanotubes possessed similar pathogenic effects as asbestos fibers leading to recruitment of inflammatory cells and the thickening of mesothelioma in the lining of abdominal cavity after an intraperitoneally injected dose of 50 μg/mouse of MCNT. However, the underlying molecular mechanism of these pathogenic effects remains to be elucidated.

The IL-1 family cytokines IL-1α, IL-1β and IL-18 are important mediators of inflammatory responses. Their functions include both systemic and local effects such as activation of the production of other pro-inflammatory cytokines such as IL-6, induction of fever, recruitment of immune system cells

ABSTRACT Carbon nanomaterials (CNM) are targets of great interest because they have multiple applications in industry but also because of the fear of possible harmful heath effects of certain types of CNM. The high aspect ratio of carbon nanotubes (CNT), a feature they share with asbestos, is likely the key factor for reported toxicity of certain CNT. However, the mechanism to explain this toxicity is unclear. Here we investigated whether different CNM induce a pro-inflammatory response in human primary macrophages. Carbon black, short CNT, long, tangled CNT, long, needle-like CNT, and crocidolite asbestos were used to compare the effect of size and shape on the potency of the materials to induce secretion of interleukin (IL) 1-family cytokines. Our results demonstrated that long, needle-like CNT and asbestos activated secretion of IL-1β from LPS-primed macrophages but only long, needle-like CNT induced IL-1α secretion. SiRNA experiments demonstrated that the NLRP3 inflammasome was essential for long, needle-like CNT and asbestos-induced IL-1β secretion. Moreover, it was noted that CNT-induced NLRP3 inflammasome activation depended on reactive oxygen species (ROS) production, cathepsin B activity, P2X$_7$ receptor, and Src and Syk tyrosine kinases. These results provide new information about the mechanisms by which long, needle-like materials may cause their harmful health effects. Furthermore, the techniques used here may be of use in future risk assessments of nanomaterials.

KEYWORDS: asbestos · carbon nanomaterials · cytokine · inflammation · interleukin · macrophage · NLRP3 inflammasome

to the site of injury or inflammation and induction of apoptosis. IL-1α and IL-1β proteins bind to the same receptor whereas IL-18 has its own receptor. The regulation and function of IL-1α are not clearly understood but its precursor is known to be released from cells undergoing necrosis. IL-1α precursor, unlike those of IL-1β and IL-18, is biologically active.[5] The proteolytic processing of IL-1α is less well understood whereas tightly regulated IL-1β and IL-18 maturation and secretion mechanisms have been examined in some detail.[6,7] IL-1β and IL-18 precursor proteins are processed to mature proteins by autoactivated caspase-1 enzyme which is closely associated with inflammasome activation.[8] Inflammasomes consist of
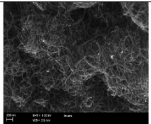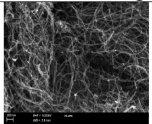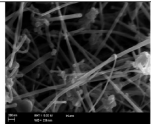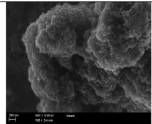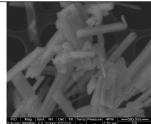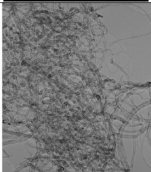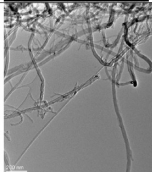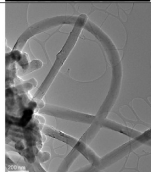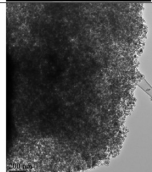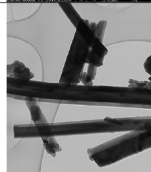
TABLE 1. Specification of the Used Nanomaterials and Crocidolite Asbestos[a]

	Short MWCNT	Long Tangled MWCNT	Long Needle-Like MWCNT	Carbon Black	Asbestos
Tradename	Baytubes C 150 HP	MWCNT 8-15nm OD	Mitsui MWCNT-7	Printex® 90	Crocidolite asbestos
Manufacturer	Bayer Material Science	Cheaptubes Inc.	Mitsui&Co, Ltd.	Evonik Industries	Pneumoconiosis Research Centre
Characteristics provided by manufacturer	OD 5-20nm Length 1->10µm	OD 8-15nm Length10-50µm SSA 233m^2/g	OD >50nm Length ~13µm	Average size 14nm SSA 300m^2/g	Av. diameter 180nm Length 4,6µm
SEM Morphology (Measure bar 200 nm, except for asbestos 500nm)					
TEM Morphology (Measure bar 200nm)					
Composition measured by TEM+EDS (Average of five measurements)	Carbon content >99wt% Residual catalyst metal (Co) content <0.2wt%	Carbon content >99wt% Residual catalyst metal (Co, Fe, Ni) content in total <0.5wt%	Carbon content >99wt% Residual catalyst metal content < the detection limit 0.1wt%	Carbon content ~100wt%	N.A.

[a] Morphology of materials by electron microscopy (SEM and TEM). Size, *i.e.*, diameters and lengths, found in the table as provided by vendor. Compositional analysis shown is average of five separate EDS analysis.

an adapter molecule (ASC) containing a CARD domain and a pattern recognition receptor (PRR) that belongs to either the NLR or the PYRIN receptor gene family. Caspase-1 activating complexes include NLRP3,[9] NOD2/NLRP1,[10] IPAF/NAIP5,[11,12] and AIM2 inflammasomes.[13] The NLRP3 inflammasome is the most important activator of IL-1β and IL-18 processing and secretion, and its activation has been shown to be triggered by many different signals including pathogen-associated molecular patterns (PAMPs) and danger associated molecular patterns (DAMPs). Certain endogenous DAMPs such as ATP,[14] monosodium urate crystals (MSU),[15] and cholesterol crystals[16] are recognized activators of the NLRP3 inflammasome. These DAMPs trigger an intracellular cascade that leads to the activation of the NLR protein complex. For example, ROS formation and lysosomal damage leading to the release of cathepsin B to cytosol are associated with NLRP3 inflammasome activation.[17,18] However, the precise mechanisms involved in the activation of the NLRP3 inflammasome are still unclear.[19]

It has been recently reported that particulate materials and asbestos are able to activate the NLRP3 inflammasome.[18,20,21] In the current work, we studied the ability of different carbon nanomaterials and crocidolite asbestos to induce pro-inflammatory effects in human primary macrophages. The results suggest that long, needle-like CNT are able to activate the NLRP3 inflammasome in a manner similar to that of asbestos. The NLRP3 inflammasome activation caused by long, needle-like MCNT depends on P2X$_7$ receptor and cathepsin B activation, ROS production, and Src and Syk tyrosine kinases, triggering profound IL-1β production.

RESULTS

Long, Needle-like Carbon Nanotubes Induce IL-1β Maturation and Secretion from Human Primary Macrophages. To study the potential of different carbon nanomaterials (CNM) to induce secretion of the IL-1 family cytokines, we chose 4 CNM with different physical properties as well as crocidolite asbestos (Table 1) and compared their effects on cytokine secretion on human primary macrophages.

An exposure with CNM or asbestos without macrophage priming did not induce any IL-1α or IL-1β secretion from human macrophages (data not shown). IL-1α secretion was strongly induced when LPS-primed primary macrophages were exposed to long, needle-like CNT. In contrast, other types of CNM and asbestos were weak inducers of IL-1α secretion (Figure 1A). The pro-IL-1β is not continuously expressed in the cytoplasm, and its transcription is known to be activated after stimulation of the Toll-like receptor (TLR), for example, by bacterial lipopolysaccharide (LPS). However, a second signal is required for inflammasome complex formation and the cleavage of IL-1β into its active form.[8] In contrast to unprimed macrophages, LPS primed human macrophages secreted IL-1β after exposure to CNM or asbestos. In the comparison of the different materials, the long, needle-like CNT induced more IL-1β secretion than the other CNM or even asbestos (Figure 1B). WB analysis confirmed that macrophages release mature IL-1β after exposure to long, needle-like CNT and asbestos but not after exposure to long, tangled CNT or short CNT (Figure 1C). The same phenomenon was seen with respect to IL-18 secretion
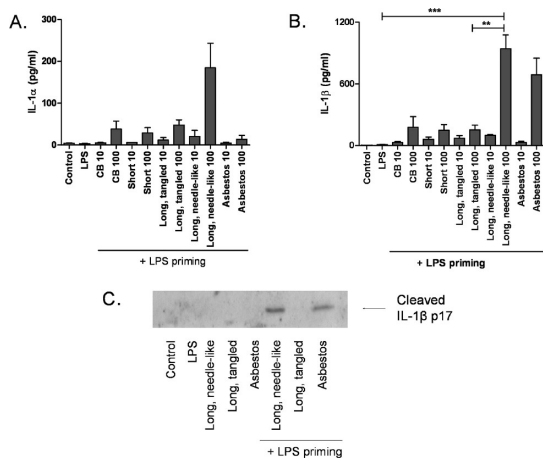
Figure 1. Needle-like carbon nanotubes induce IL-1α and IL-1β secretion from LPS-primed human primary macrophages. LPS-primed macrophages were exposed to carbon black (CB), short MCNT; long, tangled MCNT; long, needle-like MCNT, and asbestos (100 g/mL) for 6 h, cell culture supernatants were harvested and (A) IL-1α and (B) IL-1β ELISA were performed. (C) Unprimed and LPS-primed human monocyte-derived macrophages were stimulated for 6 h with long, tangled MCNT; long, needle-like MCNT and asbestos (100 g/mL). The cell culture supernatants were concentrated and IL-1β expression was analyzed by Western blotting with anti-IL-1β Abs. All values are means ± SD from three independent analyses. (∗) $P < 0.05$; (∗∗) $P < 0.01$, and (∗∗∗) $P < 0.001$.
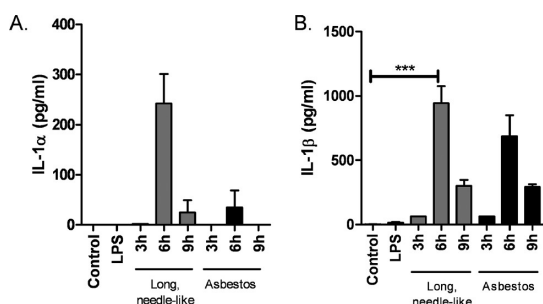

Figure 2. Kinetics of IL-1α and IL-1β secretion. LPS-primed macrophages were exposed with long, needlelike CNT and asbestos (100 μg/mL) for 3, 6, and 9 h, cell culture supernatants were collected, and (A) IL-1α and (B) IL-1β ELISA were performed. All values are means ± SD from three independent analyses. (∗) $P < 0.05$, (∗∗) $P < 0.01$, and (∗∗∗) $P < 0.001$.

(Supporting Information, Figure I). Secretion of IL-1α and IL-1β were most intense after 6 h exposure with long, needle-like CNT or asbestos, and the degradation of both cytokines began before 9 h of exposure (Figure 2). This data suggest that long, needle-like CNT are able to activate IL-1α and IL-1β secretion from human primary macrophages in an even more profound manner than asbestos fibers.

Long Carbon Nanotubes and Asbestos Are Uptaken by Primary Macrophages. Transmission electron microscopy (TEM) was utilized to study whether long, needle-like CNT; long, tangled CNT and asbestos are taken up to the primary macrophages. TEM pictures showed that all studied materials had intracellular localization in

macrophages after 6 h exposure to materials (100 μg/mL; Figure 3). All materials were observed free inside the cells; they were not seen in the vacuoles or none of the materials was seen in the nucleus of macrophages. We also performed acridine orange (AO) staining as described in Materials and Methods. Fluorescent microscopy pictures suggest treatment of macrophages with different materials causes different outcomes to the cell size and shape (Supporting Information Figure II). Macrophages treated with long, needle-like CNT and asbestos are clearly enlarged; cells also seem to be under stress conditions according to vacuoles in the cytoplasm and changes of the AO staining. In comparison macrophages treated with long, tangled CNT resemble more the nontreated cells on their size and shape and the outcome of AO staining. These results demonstrate there are no differences between uptake of materials by primary macrophages but there are differences between intracellular responses of macrophages toward different materials.

Long, Needle-like Carbon Nanotubes Activate NLRP3 Inflammasome. To clarify whether the NLRP3 inflammasome was activated in the response of the long, needle-like CNT, we performed gene silencing with NLRP3 targeting small interfering RNA in human macrophages. The NLRP3 siRNA treatment clearly decreased IL-1β secretion from human macrophages after long, needle-like CNT and asbestos exposures (Figure 4A,B). Inflammasome-mediated secretion of cytokines of IL-1 family is associated with simultaneous secretion of inflammasome components into the cell culture media. WB displayed three isoforms of the ASC molecule, the central component of the inflammasome, in the cell culture supernatants after the exposure protocol with long, needle-like CNT and asbestos (Figure 4C).

Long, Needle-like Carbon Nanotubes Activate NLRP3 Inflammasome via ROS Production and Cathepsin B Activation. ROS formation and the leakage of cathepsin B from lysosome to the cytosol are associated with the activation of the NLRP3 inflammasome. In this study, we utilized different kinds of pharmacological blockades of ROS: Antioxidants (2R,4R)-4-aminopyrrolidine-2,4-dicarboxylate (APDC) and N-acetyl-cysteine (NAC) and NADPH oxidase inhibitor diphenyleneiodonium chloride (DPI) and cathepsin B inhibitor (Ca-047-Me) to determine whether the NLRP3 activation induced by rigid, needle-like materials was dependent upon these pathways. After the inhibition, we observed impaired IL-1β secretion after long, needle-like CNT and asbestos exposures (Figure 5A,B; Supporting Information Figure III). Furthermore, WB analysis of cell culture supernatants revealed the secretion of mature cathepsin B after the exposure with long needle-like CNT and asbestos in LPS-primed macrophages (Figure 5C).

The P2X7 Receptor Activation Is Important in NLRP3 Inflammasome Activation Caused by Long, Needle-like CNT and Asbestos. It is known that the extracellular ATP gating cation
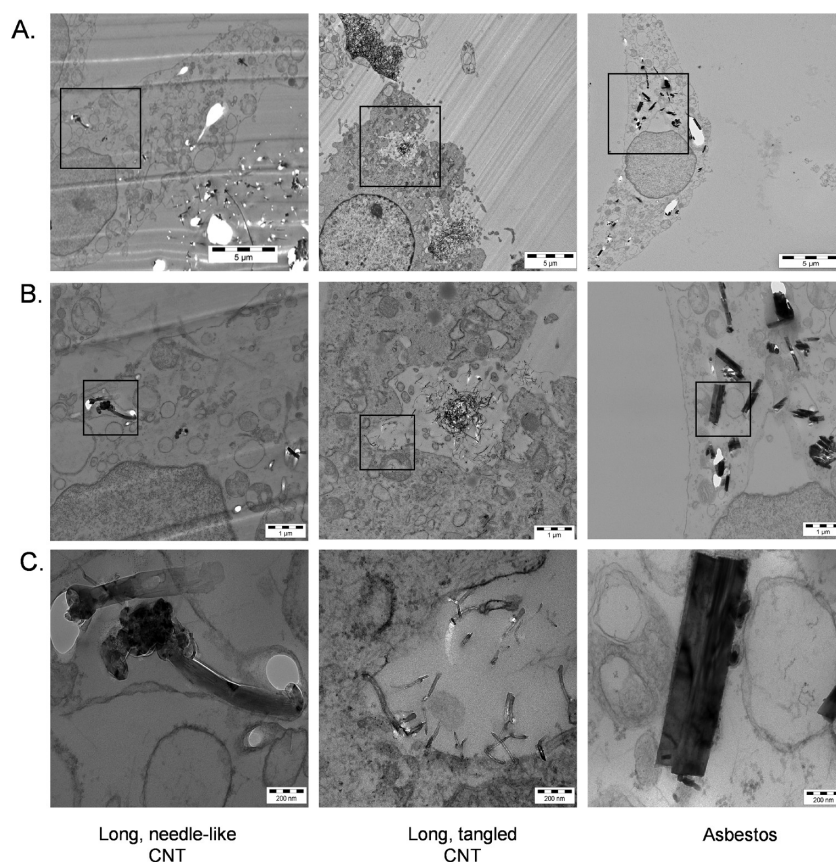
Figure 3. TEM images of human primary macrophages exposed to LPS-primed long, needle-like CNT; long, tangled CNT and asbestos (100 μg/mL) for 6 h. (A) Caption with 5 000$\times$ magnification; (B) 20 000$\times$ magnification; (C) 100 000$\times$ magnification.

channel $P2X_7$ is an important upstream activator of the NLRP3 inflammasome.[22−25] The $P2X_7$ receptor allow cations to pass through the cell membrane, for example, K+ efflux, and this is known to be associated to activation of the NLRP3 inflammasome.[26] In an attempt to understand the role of $P2X_7$ receptor in the secretion of IL-1β evoked by long, needle-like CNT and asbestos, we used both pharmacological blockade and siRNA-induced inhibition of the $P2X_7$ receptor. The $P2X_7$ receptor inhibition clearly decreased IL-1β secretion from human primary macrophages (Figure 6A) as did the siRNA treatment suggesting that the $P2X_7$ receptor is an important molecule upstream of the NLRP3 inflammasome after exposure of cells to long, needle-like CNT and asbestos (Figure 6B,C). These results demonstrate that stimulation of the $P2X_7$ receptor is essential for the activation of the NLRP3 inflammasome activation triggered by rigid, needle-like materials.

NLRP3 Inflammasome Activation after Rigid, Needle-like Materials Is Dependent on Src and Syk Tyrosine Kinase Activation. Both Src and spleen tyrosine kinase (Syk) are thought to be involved in NLRP3 inflammasome activation.[26−28] To investigate whether this pathway is important in NLRP3 inflammasome activation caused by rigid, needle-like materials, we used the Src kinase inhibitor PP2 and the Syk-kinase inhibitor SYK II. Both compounds impaired dose-dependently the production of IL-1β

evoked by long, needle-like CNT and asbestos (Figure 7). According to the results, tyrosine kinase pathways are essential for NLRP3 inflammasome activation and secretion of pro-inflammatory cytokines after exposure to either long, needle-like CNT or asbestos.

DISCUSSION

Manufacturers are utilizing different nanomaterials in a wide variety of products, and special interest has focused on technologies incorporating carbon nanomaterials (CNM). Because of their optimal physicochemical properties these rigid fibres have found a multitude of purposes. As nanomaterials (NM) become more and more widely used, it has been estimated that several million workers are being exposed to these materials, and the number of exposed consumers may reach hundreds of millions by 2014.[29] Nonetheless, it is not known whether one particular type of CNM poses a greater health risk to workers and consumers. Therefore, a careful risk-assessment is essential for assuring the safe use and handling of these materials.[30] CNM are formed from graphene and their shape and size may affect on their physicochemical properties and toxicity.[31] It has been reported that exposure to long, needle-like CNT induced severe health effects in experimental *in vivo* models but at present, the mechanisms to account for these adverse effects are unknown.[32]
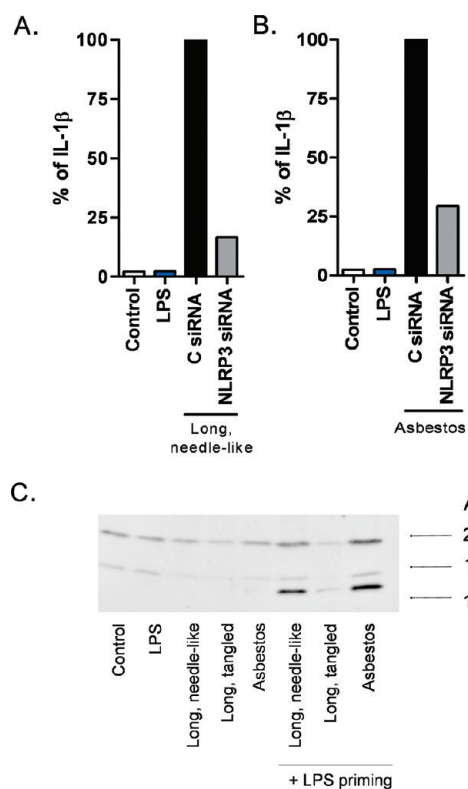
Figure 4. Needle-like CNT and asbestos activate NLRP3 inflammasome (A) Macrophages were transfected with the nontargeting siRNA control (c siRNA) or the NLRP3 siRNAs (NLRP3 siRNA) as described in Materials and Methods. LPS-primed human monocyte-derived macrophages were stimulated with A. long, needle-like CNT and B. asbestos (100 μg/mL) for 6 h, cell culture supernatants were collected and IL-1β ELISA was performed. The values are percentages of measured protein concentrations of two independent analysis where control siRNA = 100%. C. Unprimed and LPS-primed human monocyte-derived macrophages were stimulated for 6 h with long, tangled MCNT; long, needle-like MCNT and asbestos (100 μg/mL). The cell culture supernatants were concentrated and protein expressions were analyzed by Western blotting with anti-ASC Abs. (∗) $P < 0.05$, (∗∗) $P < 0.01$, and (∗∗∗) $P < 0.001$.
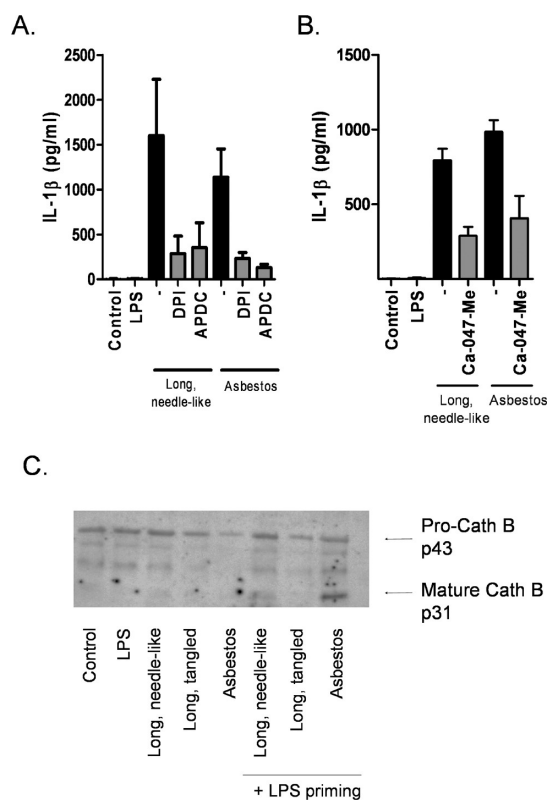
Figure 5. Needle-like CNT and asbestos induced NLRP3 inflammasome activation is dependent on ROS production and cathepsin B activation. LPS-primed human monocyte-derived macrophages were treated with long, needle-like CNT or crocidolite asbestos (100 μg/mL) in the absence or presence of (A) ROS inhibitor NAC (10 mM) or (B) cathepsin B inhibitor Ca-047-Me (10 μM). Cell culture supernatants were harvested after 6 h of exposure and IL-1β ELISA was performed (C) Unprimed and LPS-primed human monocyte-derived macrophages were stimulated for 6 h with long, tangled MCNT; long, needle-like MCNT, and asbestos (100 μg/mL). The cell culture supernatants were concentrated, and cathepsin B secretion was analyzed by Western blotting with anti-Cathepsin B Abs. All values are means ± SD from three independent analyses. (∗) $P < 0.05$, (∗∗) $P < 0.01$, and (∗∗∗) $P < 0.001$.

Cytokines of IL-1 family, especially IL-1α and IL-1β, are important activators of the pro-inflammatory response. The IL-1β cytokine is of particular interest because its production has been shown to be associated with autoimmune disorders and fibrosis.[20,33] Our working hypothesis was that long, needle-like CNT would be similar to asbestos in their ability to activate pro-inflammatory response. Our results revealed that pro-IL-1β is processed to active IL-1β after exposure with long, needle-like carbon nanotubes and asbestos. In contrast, short CNT or long, tangled CNT do not activate the secretion of IL-1β in a robust manner. Utilizing gene silencing it was possible to demonstrate that the NLRP3 inflammasome is critically involved in IL-1β secretion from macrophages. Interestingly, the extent of the IL-1α secretion evoked by long, needle-like CNT was greater than could be achieved with asbestos. The functions and regulation of IL-1α are not clearly understood, but it does not require proteolytic processing by caspase-1 to be secreted.[5] Instead, the NLRP3 inflammasome activates caspase-1 which in turn regulates unconventional secretion pathways leading to IL-1α secretion.[34] In a recent study it was shown that IL-1α and IL-1β secretions were induced by exposure to nano-TiO$_2$ and nano-SiO$_2$.[35] However, our study is the first to show that also long, needle-like CNT can activate the NLRP3 inflammasome and induce a robust secretion of both IL-1α and IL-1β cytokines.

Both long, needle-like and long, tangled CNT as well as asbestos are uptaken by primary macrophages. Previously, it has been suggested MCNT are able to enter the cells passively through the membranes.[36,37] Our data supports these findings as materials are located free in the cytosol instead of vesicular structures. In the microscopic evaluation of cells after the exposure with different materials, macrophage size and shape is drastically changed compared to untreated
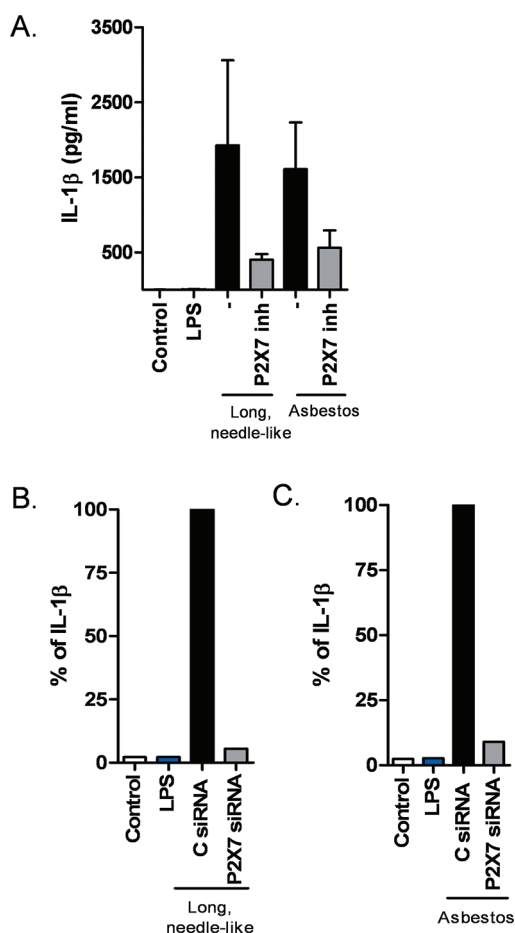
Figure 6. P2X$_7$ receptor activation is an upstream signal for NLRP3 inflammasome activation. (A) LPS-primed human monocyte-derived macrophages were treated with long, needle-like CNT or crocidolite asbestos (100 μg/mL) in the absence or presence of P2X$_7$ inhibitor (1 μM). Cell culture supernatants were harvested after 6 h of exposure and IL-1β ELISA was performed. Macrophages were transfected using the nontargeting siRNA control (c siRNA) or the P2X$_7$ siRNAs (P2X$_7$ siRNA) as described in Materials and Methods. LPS-primed human macrophages were stimulated with (B) long, needle-like CNT or (C) asbestos (100 μg/mL) for 6 h, cell culture supernatants were harvested, and IL-1β ELISA was performed. Values are percentages of measured protein concentrations of two independent analysis where control siRNA = 100%. ($*$) $P < 0.05$, ($**$) $P < 0.01$, and ($***$) $P < 0.001$.

Figure 7. Src and Syk −tyrosine kinases are essential for NLRP3 inflammasome activation. LPS-primed human monocyte-derived macrophages were treated with long, needle-like CNT or crocidolite asbestos (100 μg/mL) in the absence or presence of A. Src kinase inhibitor PP2 (1, 5, and 10 μM), B. Syk-kinase inhibitor SYK (1 and 5 μM) Cell culture supernatants were harvested after 6 h of exposure and IL-1β ELISA was performed. All IL-1β values are means $\pm$ SD from two independent analyses. ($*$) $P < 0.05$, ($**$) $P < 0.01$, and ($***$) $P < 0.001$.

controls suggesting cellular stress response toward ingested materials. There was a clear difference between macrophage morphology after exposure to long, needle-like CNT and long, tangled CNT suggesting that long, needle-like CNT are more harmful to macrophages resembling asbestos fibers. To find out the mechanisms of this different response, more specific studies about the molecular mechanisms behind the phenomenon were performed. ROS production is known to be an important upstream signal for NLRP3 activation.[21,38,39] Additionally, it has been shown that silica crystals activate the NLRP3 inflammasome by endosomal rupture followed by leakage of cathepsin B, a lysosomal enzyme previously linked with apoptotic reactions, to cytoplasm.[18,40] The material's inability to
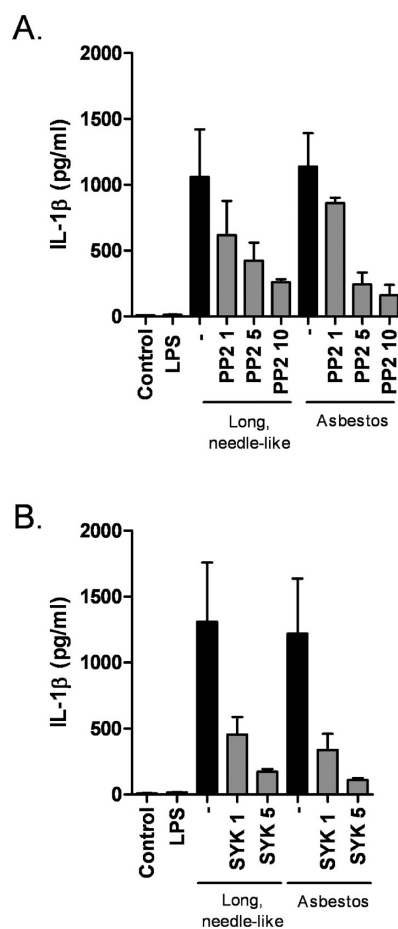
induce abiotic ROS production suggested there is no significant difference between OH radical formation caused by used materials. Also, in the present study, the treatment with both ROS and NADPH inhibitors and a pharmacological blockade of cathepsin B function causes a clear impairment in IL-1β secretion in response to the needle-like materials. Furthermore, Western blotting analysis of cell culture supernatant revealed that the mature form of cathepsin B is secreted from macrophages in response to long, needle-like CNT and asbestos. In conclusion, our results demonstrate that both NADPH oxidase-dependent production of ROS and cathepsin B have important roles in the NLRP3 inflammasome activation in response to long, needle-like CNT and asbestos independently of the material's ability to produce OH-radicals.

P2X$_7$ receptor belongs to the family of purinoreceptors for extracellular ATP. When activated, this receptor triggers a signaling cascade leading to inflammation.

Stimulation of P2X$_7$ receptor with ATP provokes the rapid assembly of the NLRP3 inflammasome complex, resulting in IL-1β secretion in LPS-primed macrophages.[22,25] Our current data show that IL-1β secretion in LPS-primed macrophages in response to long, needle-like CNT and asbestos is dependent on the P2X$_7$ receptor. Both pharmacological inhibition as well as gene silencing of P2X$_7$ receptor with siRNA abolishes IL-1β secretion in response to long, needle-like CNT and asbestos. It is known that tyrosine kinase activation is essential for P2X$_7$ receptor functions.[41] In addition, Shio et al.[42] reported that malarial hemozoin activates the NLRP3 inflammasome through Lyn, a member of Src kinase family, and Syk kinase phosphorylation suggesting these tyrosine kinases are important signaling molecules in the control of IL-1β maturation.[26,42,43] This study provides clear evidence that both Src and Syk kinases are essential for NLRP3 inflammasome activation caused by long, needle-like carbon nanotubes and asbestos fibers. A pharmacological blockade of the Src kinases as well as a specific inhibitor of Syk kinases suppressed dose-dependently the secretion of IL-1β induced by long, needle-like CNT. It is known that Syk kinase is located downstream from Src, and is able to activate cathepsin B.[44] To conclude, our results demonstrate a novel link between the P2X$_7$ receptor, Src and Syk tyrosine kinases, cathepsin B, and inflammasome activation evoked by rigid, needle-like materials.

Long, needle-like CNT have been reported to cause mesothelioma and asbestos-like granuloma formation in the peritoneal cavities of CNT exposed mice.[2,4] In addition, a recent study indicated that long, needle-like CNT can reach the subpleural tissue of lungs after inhalation exposure.[3] CNT clearance from lungs is also assumed to be impaired.[31] Long, needle-like CNT share these features with asbestos fibres and this has raised concerns about the effect of high aspect ratio nanomaterials (HARN) having highly pathogenic effects in exposed individuals.[30] Our study confirms that the long, needle-like CNT can cause potentially harmful inflammatory effects through NLRP3 inflammasome activation, whereas the short or long, tangled CNT do not have a similar effect on the pro-inflammatory machinery in vitro. Composition analysis of used materials showed high carbon content in all nanomaterials and therefore impurities are not the reason for the different activation profiles. The long, needle-like CNT acted in a manner similar to that of asbestos suggesting that material shape and size are two of the most important factors affecting their ability to cause NLRP3 inflammasome mediated pro-inflammatory responses.

It has been previously shown that secretion of IL-1β, a NLRP3 inflammasome regulated cytokine, is highly associated with autoimmune disorders and the induction of pro-inflammatory cascades leading to severe tissue injury.[32] Present findings in conjunction with recent reports suggest that activation of NLRP3 inflammasome may be a central factor mediating nanomaterial induced pro-inflammatory effects.[34,45,46] However, it should be noted, that NLRP3 inflammasome activation alone is not sufficient to lead to a dangerous phenomenon, but the presence of simultaneous infections or autoimmune disorders could increase the risk of inflammatory disorders. Thus, the investigation of the ability of NM to activate the NLRP3 inflammasome may separate potentially hazardous materials from nonharmful materials. The present results reveal new information about the underlying pathophysiological mechanisms evoked by exposure to rigid, needle-like materials. Furthermore, these findings may provide new tools for reliable risk assessment of various nanomaterials.

CONCLUSIONS

Our results suggest that long, needle-like carbon nanotubes are potent activators of inflammatory cascade by multiple mechanisms. The inflammatory effect of similar materials clearly depends on the shape of the nanomaterial, and long, needle-like CNT, which share similar characteristics as asbestos, had the most profound effects of all of these types of graphene-based materials. These data suggest that the NLRP3 inflammasome activation is an important step in the harmful health effects caused by nanomaterials. This method analyzing NLRP3 inflammasome activation evoked by nanomaterials may be a useful way to undertake a rapid scanning of toxicity of different NM in the future, and may serve as a means for supporting the risk assessment of nanomaterials. However, more research will be required to confirm the suitability of the in vitro method utilized in this study for the rapid risk assessment as a part of rational testing strategy of NM, but these results hold promise in the assessment and management of the risks of nanomaterials.

MATERIALS AND METHODS

Cells. Peripheral blood mononuclear cells (PBMCs) from healthy blood donors (Finnish Red Cross Blood Transfusion Service, Helsinki, Finland) were isolated from buffy coats by low-speed density gradient centrifugation on Ficoll-Paque Plus (Amersham Biosciences, Uppsala, Sweden). The monocytes were resuspended in RPMI-1640 (Invitrogen, Paisley, UK) with supplemental 1% penicillin–streptomycin (PEST; Invitrogen, Paisley, UK) and 1% L-glutamine (Ultraglutamine; Invitrogen, Paisley, UK). After 45 min of attachment on 6- or 12-well-plates, nonadherent cells were washed away with Dulbecco's phosphate buffered saline without Ca^{2+}, Mg^{2+} (DPBS; Lonza, Basel, Switzerland). The adherent monocytes were cultured in serum-free macrophage medium (Macrophage-SFM; Invitrogen, Paisley,

UK) supplemented with granulocyte−macrophage colony-stimulating factor (GM-CSF; BioSource, Camarillo, CA, USA) and PEST. The cells were cultured for 7 days in the respective medium to allow for differentiation of the macrophages before exposure to the nanomaterials.

Nanomaterials and Suspension Preparation. Carbon black (Printex 90) was a gift from Evonik Industries AG (Essen, Germany) as was needle-like, long multiwalled carbon nanotubes (MWCNT-7) from Mitsui&Co., Ltd. (Tokyo, Japan). Short MCNT (Baytubes C 150 HP) were provided by Bayer Material Science (Leverkusen, Germany) and long, tangled MCNT (MWCNT 8−15 nm OD) were ordered from Cheap Tubes, Inc. (Brattleboro, USA). Crocidolite asbestos was provided by Pneumoconiosis Research Centre (Johannesburg, South Africa). The size and morphology of the nanomaterials were characterized by electron microscopy (Zeiss ULTRAplus FEG-SEM, Carl Zeiss NTS GmbH, Oberkochen, Germany and FEI Quanta 200F SEM FEI Company, Eindhoven, The Netherlands and Jeol JEM 2010 TEM, Jeol Ltd., Tokyo, Japan) and their composition was analyzed by energy dispersive spectroscopy (EDSThermoNoran Vantage, Thermo Scientific, Breda, The Netherlands) attached to a Jeol JEM 2010 TEM (Table 1). Elemental composition shown in Table 1 is the average of five separate EDS analyses. Nanomaterial suspensions for experiments were prepared by weighing the materials into glass tubes and diluting them to 1 000 μg/mL stock solution with 2% fetal bovine serum in phosphate buffered saline (FBS/PBS) which was sonicated for 20 min at 30 °C. The stock solution was further serially diluted to 100 and 10 μg/mL final concentrations in serum-free macrophage medium and sonicated for 20 min at 30 °C just before cell exposures. Old media was carefully removed and replaced with new media containing the final concentrations of nanomaterials.

Electron Microscopy. PBMCs were isolated and purified as described above. After 7 days of differentation, cells were primed for 2 h with LPS and exposed with different CNT and asbestos. After the exposure period, cells were washed twice with DPBS, fixed with 2.5% glutardehyde in 0.1 M phosphate buffer, and removed from the plate by scraping. Following fixation, cells were postfixed in 1% osmium tetroxide, dehydrated, and embedded in Epon. Thin sections were collected on uncoated copper grids, stained with uranyl acetate and lead citrate and then examined with a transmission electron microscope operated at an acceleration voltage of 80 KV (JEM-1220, Jeol Ltd., Tokyo, Japan).

Fluorescent Microscopy. PBMCs were isolated and purified as described above but this time the cells were allowed to adhere onto the cover slides in 12-well plates. The cells were let to grow for 7 days after which they were primed for 2 h with LPS and exposed with long, tangled CNT, long, needle-like CNT, and asbestos for 6 h. After the exposure period, cells were washed twice with DPBS, and acridine orange (AO 0,004% in Sorensen buffer, Sigma-Aldrich) was added to the wells. After 1 min, AO was replaced with Sorensen buffer for 3 min, and this was repeated 3 times. After these washes, the cover slides with AO stained cells were placed upside-down onto the object class with a drop of Sorensen buffer. Fluorescent microscopy analysis of slides was performed by using a Zeiss Plan Apochromat 40 objective mounted on a Zeiss Axiolmager microscope (Carl Zeiss MicroImaging GmbH, Germany) equipped with an ISIS fluorescent imaging system, version 5.1 (MetaSystems GmbH, Germany).

OH Radical Formation Capacity of Materials. Determination of the intrinsic OH-radical formation capacity was determined using the benzoic acid probe which during dispersion in phosphate buffered water reacts with hydroxyl radical to form 4-HBA (4-hydroxy benzoic acid). The present method is slightly modified as compared to the proposal by Jung et al.[45] The test conditions are a simple simulation of the lung lining fluid in human lungs using pH 7.4 and 37 °C.

The test material was weighed into 2-mL Eppendorf centrifuge tubes and prewetted with 10 μL of ethanol. The particles are then suspended in ca. 1 mL of a solution of 10 mM benzoic acid and 10 mM phosphate buffer pH 7.4 to produce four different test concentrations (2, 5, 10, and 15 mg/mL). The tubes were vortexed for 10 s and placed on a vigorous orbital shaker

(IKA Vibrax, set to 1000 rpm) in an incubator at 37 °C for 96 h. After incubation, suspensions were centrifuged (20000G for 30 min at 23 °C), and 250 μL of the aqueous supernatant was transferred to a glass vial with an addition of 10 μL of 5 M HCl to optimize HPLC conditions (high performance liquid chromatography). A 25 μL portion of an acidified sample was injected into a HPLC system with UV detection (see following). For each sequence a 6 point standard curve, containing 4-HBA is prepared.

Buffered benzoic acid solutions without particles, incubated for 96 h, were used as blank samples, and NIST1649a urban dust was used as an internal positive control (in this test 5.8 ± 3.4 and 6.0 ± 3.4 nmol OH-radical/mg).

The HPLC system consisted of a Waters Pump 1525, Waters autosampler 2707, and Waters UV/visible detector 2488 and two Xterra MS 5 um-C18 (3.9×150 mm^2) columns in series. The system is controlled by the software Breeze. The mobile phases consisted of water adjusted to pH 2 with HCl (A) and acetonitrile (B) with the following eluent program: 30% B for 1 min, 30 to 80% B in 4 min, and 80% B for 1 min. 4-HBA was detected at 280 nm. Benzoic acid (>99.9%), 4-hydroxy benzoic acid (>99.9%), and acetonitrile (>99.9%) were obtained from Aldrich.

The final radical formation capacity was calculated as the slope of the dose-concentration curves taking into consideration the yield of 21.5% of 4-HBA from the reaction between OH-radical and benzoic acid. The standard deviation was the deviation around the slope in the regression curve, and the simple squared Pearson correlation was used for statistics (R^2).

Reagents. Bacterial lipopolysaccharide (LPS; *Escherichia coli* 0111:B4, Sigma-Aldrich, Schnelldoff, Germany) was used in experiments in a concentration of 100 ng/mL. Reagents used in the experiments were cathepsin B inhibitor Ca-047-Me (10 μM; Calbiochem, Darmstadt, Germany), reactive oxidative species (ROS) inhibitor *N*-acetyl-L-cysteine (NAC, 10 mM; Sigma-Aldrich), diphenyleneiodonium chloride (DPI, 1 μM; Sigma-Aldrich) and (2*R*,4*R*)-4-aminopyrrolidine-2,4-dicarboxylate (APDC, 30 μM; Sigma-Aldrich), P2X$_7$ receptor inhibitor AZ11645373 (1 μM; Sigma-Aldrich), selective inhibitor of Src-family protein tyrosine kinases PP2 (1, 5, and 10 μM; Sigma-Aldrich) and spleen tyrosine kinase (Syk)-inhibitor II (1 μM and 5 μM; Calbiochem). When inhibitors were used, they were added to the wells 1 h prior to exposure to the nanomaterials.

Small Interfering RNA Assays. After 6 d of cell culture in 12-well plates, macrophages were transfected with 200 nM nontargeting control small interfering RNA (siRNA, AllStars Negative Control siRNA, Qiagen, Valencia, CA, US), 50 nM of four different NLRP3 siRNAs (Hs_CIAS1_6, Hs_CIAS1_9; Hs_CIAS1_10, Hs_CIAS1_11; Qiagen) or 100 nM of two different P2X$_7$ siRNAs (Hs_P2RX7_1, Hs_P2RX7_2; Qiagen) using the HiPerFect Transfection Reagent (Qiagen) according the manufacturer's instruction. After 4 h of incubation with siRNAs, cell culture media was removed and 500 μL of fresh media added to the wells. At day 7, appropriate wells were primed for 2 h with 100 ng/mL of LPS, and cells were left untreated or treated with 100 μg/mL of long, needle-like MCNF or asbestos. After the exposure period, the cell culture supernatants were collected.

Western Blotting and Enzyme-Linked Immunosorbent Assay (ELISA). Processing and secretion of IL-1β, cathepsin B and ASC were analyzed by Western blot which was performed by using concentrated cell supernatants. Cell culture supernatants (6 mL) were concentrated by Amicon Ultra-15-centrifugal filter devices (Millipore, Bedford, MA, US) according to the manufacturer's instructions. After concentration, 30 μL from 240 μL of supernatants were separated on 12% SDS-PAGE at 200 V and transferred onto Immobilon-P Transfer Membranes (Millipore, Bedford, MA, US) by the Isophor electrotransfer apparatus Power-Pac Basic (Bio-Rad Laboratories) at +4 °C and 100 V for 1 h. The membranes were blocked in PBS containing 5% nonfat milk for 30 min after which they were incubated at +4 °C overnight with primary Abs. After this, the membranes were incubated at room temperature for 1 h with the appropriate HRP-conjugated secondary Abs (Dako A/S, Glostrup, Denmark). Finally, proteins were visualized by the Image Quant LAS 4000 mini quantitative imager (GE Heathcare, Fairfield, CT, US). Anti-IL-1β Ab has previously been described,[46,47] anti-Cathepsin B Ab was purchased from Calbiochem and anti-ASC Ab from Millipore. Both

human IL-1α MAX Deluxe and IL-1β Eli-pair were purchased from Diaclone (Besançor Cedex, France), and human IL-18 ELISA was purchased from Bender MedSystems (Bender MedSystems, Austria). All ELISAs were performed according to the manufacturer's instructions.

Statistical Analyses. Each macrophage sample represents a pool of separately stimulated cells from three different blood donors. ELISA results are combined from values obtained in three different stimulations, and Western blot results are representative of three independent, but similarly performed experiments unless otherwise mentioned. Data were analyzed using GraphPad Prism 4 Software (GraphPad Software Inc., San Diego, CA, USA). An unpaired t test or Mann−Whitney U-test was used to compare the differences between the groups. A P-value of <0.05 was considered to be statistically significant. In ELISA figures, data were expressed as means $\pm$ SD.

Supporting Information Available: Long, needle-like carbon nanotubes induce IL-18 cytokine secretion from human primary macrophages (Supporting Information Figure I); acridine orange staining of human primary macrophages exposed to LPS-primed long, needle-like CNT; long, tangled CNT and asbestos (Supporting Information Figure II) and IL-1β cytokine secretion induced by rigid, needle like materials is dependent on intracellular ROS-production (Supporting Information Figure III). This material is available free of charge *via* the Internet at http://pubs.acs.org.

REFERENCES AND NOTES

1. Donaldson, K.; Aitken, R.; Tran, L.; Stone, V.; Duffin, R.; Forrest, G.; Alexander, A. Carbon Nanotubes: A Review of Their Properties in Relation to Pulmonary Toxicology and Workplace Safety. *Toxicol. Sci.* **2006**, *92*, 5–22.

2. Poland, C. A.; Duffin, R.; Kinloch, I.; Maynard, A.; Wallace, W. A.; Seaton, A.; Stone, V.; Brown, S.; Macnee, W.; Donaldson, K. Carbon Nanotubes Introduced into the Abdominal Cavity of Mice Show Asbestos-Like Pathogenicity in a Pilot Study. *Nat. Nanotechnol.* **2008**, *3*, 423–428.

3. Ryman-Rasmussen, J. P.; Cesta, M. F.; Brody, A. R.; Shipley-Phillips, J. K.; Everitt, J. I.; Tewksbury, E. W.; Moss, O. R.; Wong, B. A.; Dodd, D. E.; Andersen, M. E.; *et al.* Inhaled Carbon Nanotubes Reach the Subpleural Tissue in Mice. *Nat. Nanotechnol.* **2009**, *4*, 747–751.

4. Takagi, A.; Hirose, A.; Nishimura, T.; Fukumori, N.; Ogata, A.; Ohashi, N.; Kitajima, S.; Kanno, J. Induction of Mesothelioma in p53± Mouse by Intraperitoneal Application of Multiwall Carbon Nanotube. *J. Toxicol. Sci.* **2008**, *33*, 105–116.

5. Dinarello, C. A. IL-1: Discoveries, Controversies and Future Directions. *Eur. J. Immunol.* **2010**, *40*, 599–606.

6. Chen, C. J.; Kono, H.; Golenbock, D.; Reed, G.; Akira, S.; Rock, K. L. Identification of a Key Pathway Required for the Sterile Inflammatory Response Triggered by Dying Cells. *Nat. Med.* **2007**, *13*, 851–856.

7. Kavita, U.; Mizel, S. B. Differential Sensitivity of Interleukin-1α and β Precursor Proteins to Cleavage by Calpain, a Calcium-Dependent Protease. *J. Biol. Chem.* **1995**, *270*, 27758–27765.

8. Martinon, F.; Burns, K.; Tschopp, J. The Inflammasome: A Molecular Platform Triggering Activation of Inflammatory Caspases and Processing of Pro-IL-β. *Mol. Cell* **2002**, *10*, 417–426.

9. Martinon, F.; Mayor, A.; Tschopp, J. The Inflammasomes: Guardians of the Body. *Annu. Rev. Immunol.* **2009**, *27*, 229–265.

10. Hsu, L. C.; Ali, S. R.; McGillivray, S.; Tseng, P. H.; Mariathasan, S.; Humke, E. W.; Eckmann, L.; Powell, J. J.; Nizet, V.; Dixit, V. M.; *et al.* A NOD2-NALP1 Complex Mediates Caspase-1-Dependent IL-1β Secretion in Response to Bacillus Anthracis Infection and Muramyl Dipeptide. *Proc. Natl. Acad. Sci. U.S.A.* **2008**, *105*, 7803–7808.

11. Lara-Tejero, M.; Sutterwala, F. S.; Ogura, Y.; Grant, E. P.; Bertin, J.; Coyle, A. J.; Flavell, R. A.; Galan, J. E. Role of the Caspase-1 Inflammasome in Salmonella Typhimurium Pathogenesis. *J. Exp. Med.* **2006**, *203*, 1407–1412.

12. Ren, T.; Zamboni, D. S.; Roy, C. R.; Dietrich, W. F.; Vance, R. E. Flagellin-Deficient Legionella Mutants Evade Caspase-1- and Naip5-Mediated Macrophage Immunity. *PLoS Pathog.* **2006**, *2*, e18.

13. Hornung, V.; Ablasser, A.; Charrel-Dennis, M.; Bauernfeind, F.; Horvath, G.; Caffrey, D. R.; Latz, E.; Fitzgerald, K. A. AIM2 Recognizes Cytosolic DsDNA and Forms a Caspase-1-activating Inflammasome with ASC. *Nature* **2009**, *458*, 514–518.

14. Mariathasan, S.; Weiss, D. S.; Newton, K.; McBride, J.; O'Rourke, K.; Roose-Girma, M.; Lee, W. P.; Weinrauch, Y.; Monack, D. M.; Dixit, V. M. Cryopyrin Activates the Inflammasome in Response to Toxins and ATP. *Nature* **2006**, *440*, 228–232.

15. Martinon, F.; Petrilli, V.; Mayor, A.; Tardivel, A.; Tschopp, J. Gout-Associated Uric Acid Crystals Activate the NALP3 Inflammasome. *Nature* **2006**, *440*, 237–241.

16. Duewell, P.; Kono, H.; Rayner, K. J.; Sirois, C. M.; Vladimer, G.; Bauernfeind, F. G.; Abela, G. S.; Franchi, L.; Nunez, G.; Schnurr, M; *et al.* NLRP3 Inflammasomes Are Required for Atherogenesis and Activated by Cholesterol Crystals. *Nature* **2010**, *464*, 1357–1361.

17. Halle, A.; Hornung, V.; Petzold, G. C.; Stewart, C. R.; Monks, B. G.; Reinheckel, T.; Fitzgerald, K. A.; Latz, E.; Moore, K. J.; Golenbock, D. T. The NALP3 Inflammasome Is Involved in the Innate Immune Response to Amyloid-β. *Nat. Immunol.* **2008**, *9*, 857–865.

18. Hornung, V.; Bauernfeind, F.; Halle, A.; Samstad, E. O.; Kono, H.; Rock, K. L.; Fitzgerald, K. A.; Latz, E. Silica Crystals and Aluminum Salts Activate the NALP3 Inflammasome through Phagosomal Destabilization. *Nat. Immunol.* **2008**, *9*, 847–856.

19. Schroder, K.; Tschopp, J. The Inflammasomes. *Cell* **2010**, *140*, 821–832.

20. Cassel, S. L.; Eisenbarth, S. C.; Iyer, S. S.; Sadler, J. J.; Colegio, O. R.; Tephly, L. A.; Carter, A. B.; Rothman, P. B.; Flavell, R. A.; Sutterwala, F. S. The NALP3 Inflammasome Is Essential for the Development of Silicosis. *Proc. Natl. Acad. Sci. U.S.A.* **2008**, *105*, 9035–9040.

21. Dostert, C.; Petrilli, V.; Van Bruggen, R.; Steele, C.; Mossman, B. T.; Tschopp, J. Innate Immune Activation through NALP3 Inflammasome Sensing of Asbestos and Silica. *Science* **2008**, *320*, 674–677.

22. Kahlenberg, J. M.; Dubyak, G. R. Mechanisms of Caspase-1 Activation by P2X$_7$ Receptor-Mediated K+ Release. *Am. J. Physiol. Cell Physiol.* **2004**, *286*, C1100–1108.

23. Pelegrin, P.; Surprenant, A. Pannexin-1 Mediates Large Pore Formation and Interleukin-1β Release by the ATP-gated P2X$_7$ Receptor. *Embo. J.* **2006**, *25*, 5071–5082.

24. Petrilli, V.; Papin, S.; Dostert, C.; Mayor, A.; Martinon, F.; Tschopp, J. Activation of the NALP3 Inflammasome Is Triggered by Low Intracellular Potassium Concentration. *Cell Death Differ.* **2007**, *14*, 1583–1589.

25. Riteau, N.; Gasse, P.; Fauconnier, L.; Gombault, A.; Couegnat, M.; Fick, L.; Kanellopoulos, J.; Quesniaux, V. F.; Marchand-Adam, S.; Crestani, B.; *et al.* Extracellular ATP Is a Danger Signal Activating P2X$_7$ Receptor in Lung Inflammation and Fibrosis. *Am. J. Respir. Crit. Care Med.* **2010**, *182*, 774–783.

26. Gross, O.; Poeck, H.; Bscheider, M.; Dostert, C.; Hannesschlager, N.; Endres, S.; Hartmann, G.; Tardivel, A.; Schweighoffer, E.; Tybulewicz, V.; e*et al.* Syk Kinase Signalling Couples to the NLRP3 Inflammasome for Anti-Fungal Host Defence. *Nature* **2009**, *459*, 433–436.

27. Dostert, C.; Guarda, G.; Romero, J. F.; Menu, P.; Gross, O.; Tardivel, A.; Suva, M. L.; Stehle, J. C.; Kopf, M.; Stamenkovic, I.; *et al.* Malarial Hemozoin Is a NALP3 Inflammasome Activating Danger Signal. *PLoS One* **2009**, *4*, e6510.

28. Kankkunen, P.; Teirila, L.; Rintahaka, J.; Alenius, H.; Wolff, H.; Matikainen, S. (1,3)-β-Glucans Activate Both Dectin-1 and NLRP3 Inflammasome in Human Macrophages. *J. Immunol.* **2010**, *184*, 6335–6342.

29. Shatkin, J. A.; Abbott, L. C.; Bradley, A. E.; Canady, R. A.; Guidotti, T.; Kulinowski, K. M.; Lofstedt, R. E.; Louis, G.; Macdonell, M.; Maynard, A. D. Nano Risk Analysis: Advancing the Science for Nanomaterials Risk Management. *Risk Anal.* **2010**, *30*, 1680–1687.

30. Maynard, A. D.; Aitken, R. J.; Butz, T.; Colvin, V.; Donaldson, K.; Oberdorster, G.; Philbert, M. A.; Ryan, J.; Seaton, A.; Stone, V.; *et al*. Safe Handling of Nanotechnology. *Nature* **2006**, *444*, 267–269.

31. Donaldson, K.; Murphy, F.; Schinwald, A.; Duffin, R.; Poland, C. A. Identifying the Pulmonary Hazard of High Aspect Ratio Nanoparticles to Enable Their Safety-by-Design. *Nanomedicine (London)* **2011**, *6*, 143–156.

32. Donaldson, K.; Poland, C. A. Nanotoxicology: New Insights into Nanotubes. *Nat. Nanotechnol.* **2009**, *4*, 708–710.

33. Chen, M.; Wang, H.; Chen, W.; Meng, G. Regulation of Adaptive Immunity by the NLRP3 Inflammasome. *Int. Immunopharm.* **2011**, *11*, 549–554.

34. Keller, M.; Ruegg, A.; Werner, S.; Beer, H. D. Active Caspase-1 Is a Regulator of Unconventional Protein Secretion. *Cell* **2008**, *132*, 818–831.

35. Yazdi, A. S.; Guarda, G.; Riteau, N.; Drexler, S. K.; Tardivel, A.; Couillin, I.; Tschopp, J. Nanoparticles Activate the NLR Pyrin Domain Containing 3 (NLRP3) Inflammasome and Cause Pulmonary Inflammation through Release of IL-1α and IL-1β. *Proc. Natl. Acad. Sci. U.S.A.* **2010**, *107*, 19449–19454.

36. Kostarelos, K.; Lacerda, L.; Pastorin, G.; Wu, W.; Wieckowski, S.; Luangsivilay, J.; Godefroy, S.; Pantarotto, D.; Briand, J. P.; Muller, S.; *et al*. Cellular Uptake of Functionalized Carbon Nanotubes Is Independent of Functional Group and Cell Type. *Nat. Nanotechnol.* **2007**, *2*, 108–113.

37. Sund, J.; Alenius, H.; Vippola, M.; Savolainen, K.; Puustinen, A. Proteomic Characterization of Engineered Nanomaterial-Protein Interactions in Relation to Surface Reactivity. *ACS Nano* **2011**, *5*, 4300–4309.

38. Zhou, R.; Yazdi, A. S.; Menu, P.; Tschopp, J. A Role for Mitochondria in NLRP3 Inflammasome Activation. *Nature* **2011**, *469*, 221–225.

39. Boya, P.; Kroemer, G. Lysosomal Membrane Permeabilization in Cell Death. *Oncogene* **2008**, *27*, 6434–6451.

40. Wewers, M. D.; Sarkar, A. P2X$_7$ Receptor and Macrophage Function. *Purinergic Signalling* **2009**, *5*, 189–195.

41. Shio, M. T.; Eisenbarth, S. C.; Savaria, M.; Vinet, A. F.; Bellemare, M. J.; Harder, K. W.; Sutterwala, F. S.; Bohle, D. S.; Descoteaux, A.; Flavell, R. A.; *et al.* Malarial Hemozoin Activates the NLRP3 Inflammasome through Lyn and Syk Kinases. *PLoS Pathog.* **2009**, *5*, e1000559.

42. Bradshaw, J. M. The Src, Syk, and Tec Family Kinases: Distinct Types of Molecular Switches. *Cell Signal* **2010**, *22*, 1175–1184.

43. He, J.; Tohyama, Y.; Yamamoto, K.; Kobayashi, M.; Shi, Y.; Takano, T.; Noda, C.; Tohyama, K.; Yamamura, H. Lysosome Is a Primary Organelle in B Cell Receptor-Mediated Apoptosis: An Indispensable Role of Syk in Lysosomal Function. *Genes Cells* **2005**, *10*, 23–35.

44. Morishige, T.; Yoshioka, Y.; Inakura, H.; Tanabe, A.; Yao, X.; Narimatsu, S.; Monobe, Y.; Imazawa, T.; Tsunoda, S.; Tsutsumi, Y.; *et al*. The Effect of Surface Modification of Amorphous Silica Particles on NLRP3 Inflammasome Mediated IL-1β Production, ROS Production and Endosomal Rupture. *Biomaterials* **2010**, *31*, 6833–6842.

45. Winter, M.; Beer, H. D.; Hornung, V.; Kramer, U.; Schins, R. P.; Forster, I., Activation of the Inflammasome by Amorphous Silica and TiO$_2$ Nanoparticles in Murine Dendritic Cells. *Nanotoxicology* **2010**: doi:10.3109/17435390.2010.506957

46. Pirhonen, J.; Sareneva, T.; Julkunen, I.; Matikainen, S. Virus Infection Induces Proteolytic Processing of IL-18 in Human Macrophages *via* Caspase-1 and Caspase-3 Activation. *Eur. J. Immunol.* **2001**, *31*, 726–733.

47. Pirhonen, J.; Sareneva, T.; Kurimoto, M.; Julkunen, I.; Matikainen, S. Virus Infection Activates IL-1β and IL-18 Production in Human Macrophages by a Caspase-1-Dependent Pathway. *J. Immunol.* **1999**, *162*, 7322–7329.